Mixed layer formation on the copper-deposited Ni(110) surface

T. Fukuda,* K. Iwamoto, and H. Nakayama
Department of Physical Electronics and Informatics, Graduate School of Engineering, Osaka City University, 3-3-138 Sugimoto, Sumiyoshi-Ku, Osaka 558-8585, Japan

K. Umezawa
Faculty of Liberal Arts and Sciences, Osaka Prefecture University, 1-1 Gakuen-cho, Naka-Ku, Sakai, Osaka 599-8531, Japan
(Received 24 June 2008; revised manuscript received 14 September 2008; published 20 November 2008)

We studied initial Cu overlayer formation on the Ni(110) surface by scanning tunneling microscopy (STM) in an ultrahigh vacuum. Initially, deposited Cu displaces the top Ni layer, forming two-dimensional Cu-Ni alloy on the substrate. The Cu atom embedded into the top layer was depressed in the STM image. The depression due to the lack of Ni 3*d*-derived surface local density of states was confirmed by the first-principles calculation. Ni atoms squeezed out from the top substrate layer agglomerated in the anisotropic Ni island along the close-packed $[1\bar{1}0]$ direction. Further Cu deposition resulted in a Cu-Ni mixed island. Quantitative measurement of the Cu fraction on the substrate showed that 0.71 ± 0.04 of deposited Cu was embedded in the top Ni layer, whereas significant Cu enrichment was seen on the island.

DOI: 10.1103/PhysRevB.78.195422 PACS number(s): 68.37.Ef, 68.43.Mn, 68.47.Fg, 82.37.Np

I. INTRODUCTION

Metal alloys at the surface are sometimes remarkably different from their bulk counterparts, and a wide variety of surface alloys and surface intermetallic superstructures have been revealed.[1] In some cases, immiscible combinations of metals in the bulk phase are miscible only within a single atomic layer. Au and Ag on Ni (Refs. 2 and 3) and Ag on Cu (Refs. 4 and 5) are such examples, and a great deal of attention has been focused on these bulk immiscible but surface miscible alloys. For the bulk miscible alloys, on the other hand, although preferential surface segregation of one of the constituent metals has been intensively studied so far, intermixing at the surface region has attracted less attention despite its technological importance. For example, both Cu and Ni form fcc crystal with only a 2.6% larger lattice constant for Cu than that of Ni, and they form a homogeneous solid solution by mixing without any ordered alloy. These alloys are indispensable for industry and they have been extensively employed as corrosion-resistant plumbing for sea water and various coins, known as cupronickel. The atomic composition of Cu-Ni alloys at the surface has been thoroughly studied for decades in terms of preferential Cu segregation for polycrystalline and single-crystal samples with various crystallographic orientations.[6,7] For epitaxial overlayer formation on pure single crystals, most studies have been devoted to Ni thin films on Cu substrates because of their unique magnetic properties.[8] However, the inverse case, i.e., Cu overlayers on Ni surfaces, has been less studied and only a few works have been performed.

The early study of Cu thin-film formation on the Ni(001) surface showed an initial pseudomorphic growth up to 0.8 nm followed by strain relief by introducing misfit dislocation.[9] Scanning tunneling microscopy (STM) study of the Cu/Ni(001) revealed that some of the first layer Cu atoms were shifting laterally by $1/\sqrt{8}$ lattice constant along the $\langle 110 \rangle$ directions and thereby protruded from the surface layer, resulting in the lateral relaxation of lattice-mismatched Cu overlayer.[10,11] By increasing the number of Cu overlayers, this protrusive stripe grew in width forming {111} internal facets in the Cu film, in agreement with Auger-electron diffraction (AED),[12] x-ray photoelectron diffraction (XPD),[13–15] and surface x-ray diffraction.[16] For these studies, there was no indication of intermixing or roughening at the interface between the Ni substrate and Cu overlayers, therefore, the Ni(001) substrate was assumed to be intact even after Ni overlayer formation. For the Cu/Ni(111) surface, the perturbed $\gamma\gamma$ angular correlation (PAC) of ^{111}In (Ref. 17) and the x-ray photoelectron spectroscopy of CO titration[18,19] also showed no significant mixing of Cu into the Ni substrate even after annealing at 800 K. In contrast to these faces, photoelectron spectroscopy (PES) combined with ion scattering spectroscopy (ISS) for Cu/Ni(110) exhibited significant Cu/Ni mixing even at room-temperature deposition.[20,21] Unlike the (111) and (001) faces, the arrangement of surface atoms of the Ni(110) 1×1 structure is relatively open and the coordination of the top layer atoms is smaller than other low-index faces. Therefore, it would be easy to exchange the substrate atoms to the deposited Cu at low temperatures. However, mixing of the deposited Cu into the Ni substrate is counterintuitive because the Cu surface is energetically more stable than that of the Ni surface and thereby Cu will be segregated on the surface. Lack of microscopic information on the Cu/Ni(110) surface prevents us from understanding the detailed mechanism of the intermixing between deposited Cu and the Ni substrate.

Here we address the initial Cu deposition on the Ni(110) surfaces with scanning tunneling microscopy in an ultrahigh vacuum, particularly focusing on the first overlayer formation. Individual surface Ni and Cu atoms could be well discriminated due to the large difference in the surface local density of states (LDOS), which is confirmed by the first-principles calculation. This enabled us to quantitatively measure the Cu/Ni ratio on the substrate and the overlayer. The Cu fraction on the substrate exhibited a linear dependence with the Cu deposition, indicating that a part of the deposited

Cu was embedded into the top layer by displacing substrate Ni atoms. The Cu/Ni replacement was observed during the successive STM image acquisition at room temperature, indicating that the replacement is a dynamic process even after Cu deposition. The Ni atoms squeezed out from the substrate and residual Cu that does not displace substrate Ni formed a quasi-one-dimensional (quasi-1D) island on the surface. By the quantitative Cu/Ni measurements of the island, the Cu fraction was initially suppressed, but for more than 0.2 ML Cu deposition, it became higher than what is expected from the diffusion coming from the substrate and direct deposition onto the island. This indicates that the buried Cu underneath the island is partly lifted into the top surface layer, resulting in the Cu rich island.

II. EXPERIMENTAL

Experiments were performed with an Omicron ultrahigh vacuum scanning tunneling microscope (UHV-STM) equipped with a sputter ion gun and low energy electron diffraction (LEED). The base pressure of 4×10^{-9} Pa was maintained with a 230 L ion pump and a titanium sublimation pump. A 10 mm diameter and 1 mm thick Ni(110)-oriented single-crystal sample was mounted on a molybdenum plate, and it was repeatedly cleaned by Ar^+ sputtering at 2 keV and annealing at 1050 K by radiative heating placed behind the plate. The final cleaning was performed by a 1 keV sputtering and subsequent annealing at 770 K for 10 min with pressure less than 3×10^{-8} Pa. This treatment enables a sharp 1×1 LEED pattern as well as clean 1×1 structure in the STM images. Typical defect density was less than 0.4% of the 1×1 unit, examined by atom-resolved STM images. Cu with 99.9999% purity was deposited with a tungsten conical basket with a LN_2-cooled shroud. During Cu deposition, chamber pressure remained below 1.0×10^{-8} Pa. The Cu coverages were determined by wide scan STM images. Because of the initial long diffusion of deposited Cu, the area of the island was found to be slightly reduced from the expected amount of deposition. We determined this missing coverage by the incremental Cu deposition with a fixed time and measured the increasing in the island area and added them to all the data. This causes an ambiguity of coverage determination of about ±0.02 ML. A Cu deposition rate of $5\times10^{-3}-3\times10^{-2}$ ML/s was calibrated with the above technique. The reported Cu coverages are relative to the density of the substrate Ni(110) surface (1 ML Cu=1.13×10^{15} atoms/cm^2). All Cu deposition and STM observations were performed at room temperature. STM images shown below are constant current topography with typical sample bias of $V_s=2-20$ mV and tunneling current of $I_t=1-20$ nA.

III. RESULTS AND DISCUSSION

A. STM observation

The surface morphology for the initial Cu deposition is depicted in Fig. 1. Similar to Ni deposition,[22] the Cu-deposited surface exhibits highly anisotropic islands with a few atomic widths and more than 80 nm long along the close-packed $[1\bar{1}0]$ direction. Even monatomic-width islands were sometimes found at the very early stage of Cu deposition, but these islands evaporated within a few hours and they were not stable at room temperature. An atom-resolved image of stable 1D islands is shown in Fig. 2. For this particular image, four atomic rows can be resolved for both islands. The heights of these islands were 129 ± 30 pm, close to the monoatomic layer height of 124 pm. The ends of these islands are fuzzy, indicating that mobile atoms frequently attach and detach during scanning, whereas side edges of the islands are relatively well resolved. Both on the islands and on the substrate, defectlike depressions with an atomic dimension were seen, suggesting Cu/Ni replacement similar to an Au-deposited surface.[2]

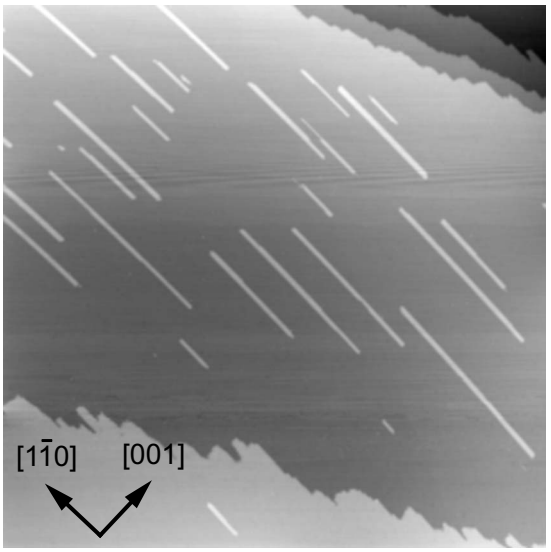

FIG. 1. Typical initial islands of 0.11 ML Cu-deposited surface, acquired with $V_s=15.2$ mV and $I_t=7.9$ nA. Scanning area is 200×200 nm^2.

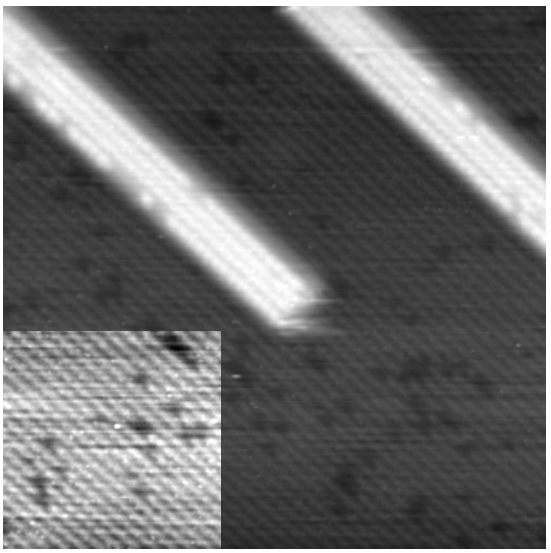

FIG. 2. A part of Fig. 1. Scanning area is 15×15 nm^2. $V_s=7.2$ mV and $I_t=7.9$ nA. Enhanced contrast at the lower left shows atomic size defects.

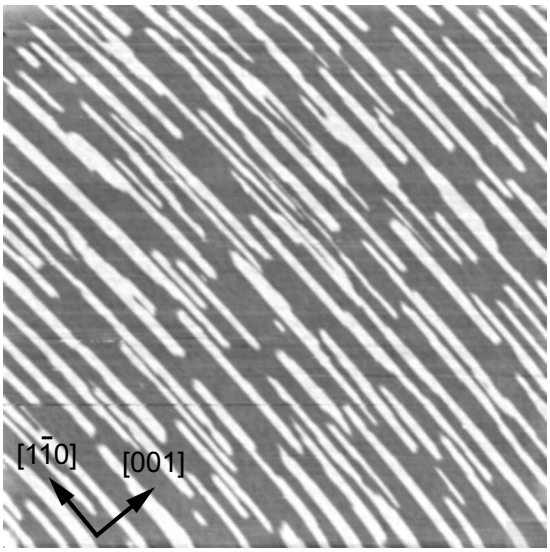

FIG. 3. 0.41 ML Cu-deposited surface. V_s=19 mV and I_t=0.6 nA. Scanning area is 200×200 nm^2.

By further Cu deposition, the number of islands and their widths were increased. A 0.41 ML Cu deposited surface and corresponding magnified image is shown in Figs. 3 and 4, respectively. The number of islands was drastically increased and their widths were also increased although they were still anisotropic along the [1$\bar{1}$0] direction. Some islands coalesced to increase their widths further. The atom-resolved image shown in Fig. 4(a) exhibits an atomic size bright feature on the island. As shown in Fig. 4(b), the protrusion of the bright site was about 60 pm higher than the surrounding area. The height of the protrusion measured from the substrate level was 130 ± 70 pm, close to but slightly higher than the monoatomic layer height. On the substrate, the depressed sites were again seen and their number increased according to the Cu deposition. The depth of the depression was 50 pm from the substrate 1×1 structure as shown in Fig. 4(c). The registry of these protrusions and depressions exactly coincides with the surface 1×1 unit both on the island and substrate, respectively, and their heights are far below the atomic size. Thus they are not due to adsorbates such as residual gas nor contamination, but they are due to the electronic origin, i.e., the increasing or decreasing in the surface local density of states. Ni 3*d* electrons significantly contribute to the LDOS near E_F, whereas Cu LDOS mainly originate from broad 4*s* bands around E_F.[23] Therefore, the surface LDOS of Cu should be smaller than that of Ni, and the embedded Cu site will be depressed in the constant current topography. Conversely, if Ni is surrounded by Cu atoms, it would be protrusive unless Ni 3*d* orbitals are filled by surrounding Cu 4*s* electrons. The depression on the substrate would, therefore, be the embedded Cu in the topmost Ni(110) layer, and the protrusion on the island would be due to Ni surrounded by Cu. The height of the protrusion on the island, measured from the substrate level, should be the monoatomic layer height. Referring to the enthalpy change by Cu mixing into bulk Ni, the energy increase is only +0.13 eV, which is considerably smaller than those of Au (+0.34 eV).[5] Therefore, the Cu will be much more easily intermixed to the Ni surface layer than Au. We should note that no contrast reversal was seen for the depression, which is occasionally observed on other embedded metals.[2,24,25] The protrusions and depressions were quite reproducible irrespective of the tip condition and the surface cleanliness.[26]

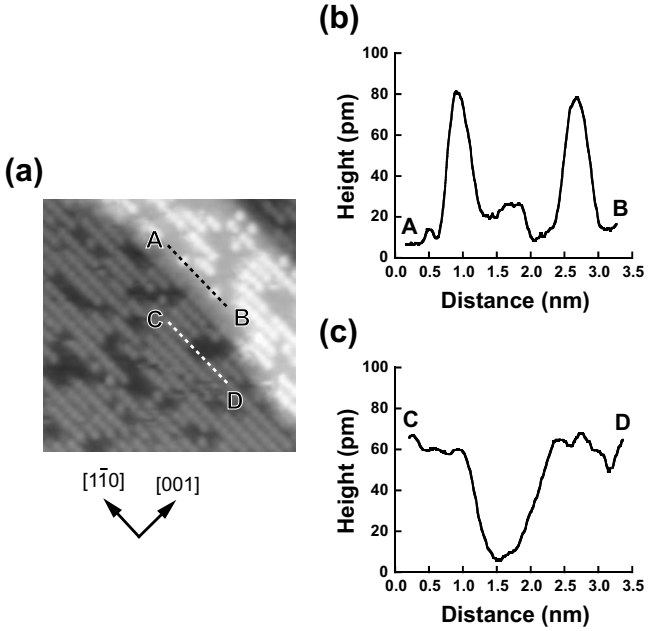

FIG. 4. (a) Atom-resolved image of the 0.41 ML Cu-deposited surface. V_s=5.3 mV and I_t=9.9 nA. Scanning area is 7.5×7.5 nm^2. Cross sections at *AA*′, and *BB*′ are shown in (b) and (c), respectively.

We noticed that these protrusions and depressions due to the Cu/Ni intermixing were not static at room temperature. Two successive STM snapshots for the same area taken 99 s apart are shown in Figs. 5(a) and 5(b), respectively. In order to show both substrate and island in one image, contrast of the substrate (upper right part) and island (lower left part) is separately adjusted. Both Figs. 5(a) and 5(b) have similar numbers of protrusions and depressions on the island (lower left) and on the substrate (upper right), respectively, but their geometry was partly different. To show their difference more clearly, we took a difference image between Figs. 5(a) and 5(b), and it is shown in Fig. 5(c). When the bright site in Fig. 5(a) became dark in Fig. 5(b), the site is represented as bright in Fig. 5(c), and vice versa. This dynamic exchange of the surface Cu/Ni geometry indicates that some Cu and Ni adatoms are always migrating on the surface, and they are frequently replacing the surface atoms. Because almost similar numbers of bright and dark sites are seen between Figs. 5(a) and 5(b), the average numbers of Cu and Ni will not be changed even though they are dynamically migrating. We tried to discriminate whether this dynamical effect is caused by the STM tip, but we could not find any systematic dependence of the migration for the tunnel resistances between 16.3 MΩ and 166 kΩ, which correspond to the bias voltage range of 2.2–20.6 meV and the tunneling current of 1.1–13.2 nA for positive and negative sample biases although the movements were slightly reduced above 4.5 MΩ. Therefore, the structural fluctuation seen in the STM images will be

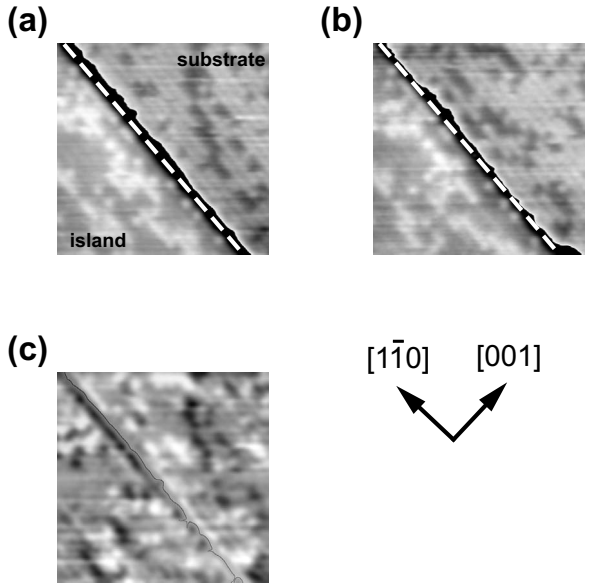

FIG. 5. Two successive images for the 0.54 ML Cu-deposited surface. Image (b) was taken 99 s after (a) with the same area. The monoatomic layer high island and the substrate are, respectively, shown in the lower left and upper right and they are separated by a broken line. In order to show both island and substrate in one image, contrast is independently adjusted, resulting in an artificial dark line at the step edge region. V_s=3.1 mV and I_t=11.2 nA for both images. Scanning areas are 7.5×7.5 nm^2. The difference image between (a) and (b) is shown in (c).

caused by the thermal fluctuation rather than the tip-induced effect. The migration of individual adatoms on the Ni(110) surface was indeed observed by field ion microscopy (FIM) even at 146 K, where the Ni adatom displaces along the [1$\bar{1}$0] and [001] directions.[27] Furthermore, the exchange of Pt adatoms with the substrate Ni of the Ni(110) surface was also seen previously at 105 K.[28] Thus, the room-temperature migration and the exchange of Cu/Ni are not surprising.

B. Image simulation of Cu-embedded Ni(110) surfaces

In order to interpret the atomic size depressions and protrusions seen in the STM images, we simulated these STM images for the Cu-embedded Ni(110) surface. We employed the first-principles calculation code based on the density-functional theory.[29,30] Projector-augmented wave method (PAW) was used for the Ni and Cu pseudopotentials, and the spin-resolved local-density functional was corrected by the generalized gradient approximation (GGA). Calculation for bulk Ni showed that the lattice constant and the cohesive energy were reproduced, respectively, within 0.2% and 2.0% of the experimental values with the energy cutoff of 24.8 Ry. With this lattice constant, we constructed the (110)-oriented slab structure with a 2×2 unit cell, six layers in depth, and a 1.0 nm vacuum gap. The top view of the atomic geometry of the Ni(110) surface and the unit cell employed in this calculation are schematically represented in Fig. 6(a). We used the Methfessel-Paxton method and optimized the smearing energy width to be σ=0.12 eV. By compromising the number

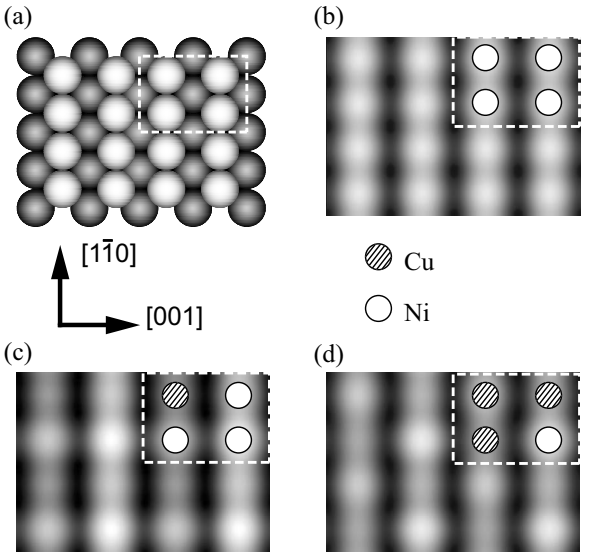

FIG. 6. (a) Atomic geometry of the Ni(110) surface. The 2×2 unit cell employed for the calculation is shown as a broken square. [(b)–(d)] Simulated STM image of the Ni(110) surface. (c) One of the top atoms is replaced with Cu, and (d) three of the top atoms are replaced with Cu.

of k points in the reciprocal lattice and allowable calculation time, we chose k mesh of 9×7, approximately 1.3 nm^{-1} along the surface. This corresponds to 20 irreducible k points for D_2^h symmetry. All atoms except for the bottom layer were fully relaxed until the force below 0.2 eV/nm, and self-consistent energy was itinerated until it converged to 10 μeV. In order to simulate the STM images, partial charge distribution of the surface atoms within the energy range of E_F and E_F-0.05 eV was sampled, and the height of the equi-charge density was mapped as a gray scale.

Figures 6(b)–6(d) are the simulated STM images for the Ni(110) surface [Fig. 6(b)] and Cu-embedded Ni(110) surfaces [Figs. 6(c) and 6(d)]. The simulated image for the Ni(110)1×1 surface in Fig. 6(b) exhibits corrugation exactly coinciding with the top atoms. By replacing one of the topmost Ni atoms with Cu, a clear depression at the Cu sites is seen, as shown in Fig. 6(c). This is due to the lack of unfilled 3d orbitals for the Cu atom site and, therefore, decreasing surface LDOS near E_F. Interestingly, the atomic position of the embedded Cu atom was 12 pm higher than surrounding Ni atoms. Therefore, the depression seen in Fig. 6(c) is not a geometric origin. For the reverse case, i.e., one Ni atom is surrounded by three Cu atoms, the surface exhibits a protrusion at the Ni site as shown in Fig. 6(d). This again indicates that the unfilled 3d orbitals are confined to the embedded Ni atom. We should note that Ni 3d bands will not be completely filled by adjacent Cu 4s electrons because the number of Cu atoms is smaller than the critical number.[31] We further find a diagonal Cu to the Ni site is slightly brighter than other Cu atoms in Fig. 6(d). Because the height difference among topmost Cu atoms was within 1 pm, the contrast is again due to the electronic effect rather than the geometrical height difference. The details of the calculation and atomic geometries of the Cu/Ni(110) surface will be published elsewhere.[32]

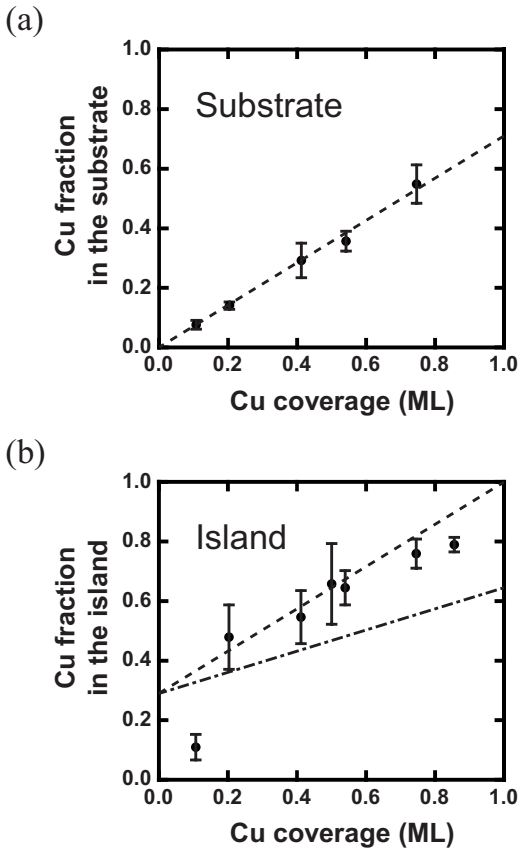

FIG. 7. (a) Cu fraction on the substrate as a function of Cu coverage. Linear fitting is represented by a broken line. (b) Cu fraction on the island as a function of Cu coverage. The dashed dotted line is for the kinetic model with Eq. (4), whereas the broken line is for the Cu lifting model Eq. (5).

C. Quantitative Cu fraction on the substrate and the island

In order to clarify the mechanism of Cu/Ni mixing on the Cu deposited Ni(110) surface in detail, the numbers of Cu atoms on the substrate and on the island were measured as a function of the surface coverage according to the image simulation as a guide for the Cu/Ni discrimination. About 450 to 12 000 atomic sites were examined for each Cu deposition on the substrate and the island independently, and fractions of Cu atoms were measured for respective regions. The summary of the measurement is depicted in Fig. 7. Error bars are due to the standard deviation of the Cu fraction in each STM image, typically 10×10 nm^2, for both substrates and islands. On the substrate, the number of Cu atoms almost linearly increases with the amount of Cu deposition. For the coverage more than 0.75 ML, it was progressively difficult to acquire atom resolved images on the substrate because the substrate became narrower due to the surrounding island. We could fit the Cu fraction with linear function with the coefficient 0.71 ± 0.04, markedly below unity, contrasted with Au deposition, where the probability of displacing substrate Ni is almost unity for low coverages.[2] On the island, however, Cu atoms are initially negligible as shown in Fig. 2, but the amount was remarkably boosted for more than 0.20 ML Cu deposition. About half of the constituent became Cu, and gradual increase in the Cu fraction follows for further Cu deposition. This behavior can be seen in Fig. 4, where more than half of the atoms on the island are depressed Cu. The distribution of Cu seems to be random both on the substrate and islands, with no clustering or phase-separation behavior such as is seen for Au/Ni(110).[2] Furthermore, even though the initial islands consist of almost pure Ni (see Fig. 2), the distribution of Cu/Ni became random for further deposition. This indicates that the initial narrow Ni islands along the close-packed $[1\bar{1}0]$ direction are completely destroyed by mixing of further Cu deposition. Because initial islands such as shown in Fig. 1 are larger than the critical nucleus, further deposited Cu should be condensed around the preexisting islands. Thus, the complete randomization of the Cu/Ni site on the island also indicates that top layer atoms on the island and migrating adatoms replace their positions quite frequently. This randomization was indeed observed at the step edges, where no accumulation of Cu or Ni was observed. From these respects, and the fact that the Cu/Ni mixing geometry is dynamically changing as shown in Fig. 5, the measured Cu fractions on the substrate and island will be a steady state of the Cu/Ni composition, which is close to thermal equilibrium.

From the surface energy point of view, the surface should be covered with Cu rather than Ni. This is true for Cu overlayers on Ni(001) (Refs. 10–16) and Ni(111) (Refs. 17–19) surfaces, where Cu overlayers are always stable, and even in Cu-Ni alloys Cu is segregated on the surface by thermal treatment.[6,7] However, the present result apparently does not follow this simple energetics. On the Ni(110) surface, substrate Ni atoms are squeezed out from the surface site by the Cu deposition, resulting in a Cu/Ni mixed layer on the substrate, and displaced Ni atoms from the substrate should form islands on top of this mixed substrate. Part of the replaced Cu atoms must therefore be buried under the newly formed island. This is understood by extrapolating the Cu fraction of islands [Fig. 7(b)] to 1 ML, which is around 0.8–0.9 ML, less than unity. Therefore, the surface will not be fully covered by Cu for a 1 ML Cu deposition. The unexpected mixed surface formation shown here indicates that the stabilizing Cu overlayer will be partly hindered kinetically, although the Cu/Ni exchange by surface migration will play a major role for the thermalization. A similar Cu/Ni mixed surface was previously reported by ion scattering and photoelectron emission spectroscopy. Relating to the previous study employing ion scattering, even for a 1 ML Cu deposition the surface exhibited unsaturating Cu concentration.[21] For completely covering the surface with Cu overlayer, Cu coverage above 1.5 ML was required. In accordance with this, at the completion of the first overlayer, 0.1–0.2 ML of Ni will kinetically float on the surface, which is in agreement with the previous photoelectron spectroscopy result[21] and the present STM results. Although the previous report showed the mixing until 40 ML Cu overlayers,[21] it was difficult to measure the Cu concentration beyond the first overlayer because multilayer high bright features appeared on the overlayer, and the discrimination of Cu and Ni became successively difficult. The surface morphology of the multilayers will be discussed elsewhere.[33,34]

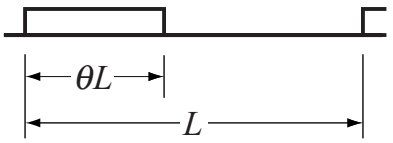

FIG. 8. Schematical one-dimensional model employed for the simulation.

In order to resolve the present Cu/Ni mixing behavior, we attempted to construct a kinetic model for Cu/Ni mixing. Because the island shape is strongly anisotropic, the island structure can be modeled by a one-dimensional periodic structure as illustrated in Fig. 8. The periodicity of the island is represented by L atomic sites with the island fraction θ, which is the same as the amount of deposited Cu with a monolayer unit. Incoming Cu flux f, denoted by the number of deposited Cu atoms to L sites per unit time, was assumed to be uniform on the substrate and the island. When the probability of displacing substrate Ni atoms by the deposited Cu is α, the Cu fraction on the substrate C_t can be written as a linear form such as

$$C_t = \alpha\theta. \tag{1}$$

The growth of the island is due to (a) the squeezed out Ni atoms and (b) unexchanged Cu atoms, both from the substrate and (c) direct Cu deposition onto the island. During the period δt, the number of Cu atoms incorporated into the island δN_i is the sum of (b) and (c), i.e.,

$$\delta N_i = f\delta t(1-\theta)(1-\alpha) + f\delta t\theta. \tag{2}$$

The average Cu fraction on the island C_i is thus written as,

$$C_i(\theta) = \frac{N_i}{L\theta} = \frac{1}{L\theta}\int_0^\theta \delta N_i, \tag{3}$$

where N_i is the number of Cu atoms incorporated into the island. Because the number of deposited Cu atoms during δt should equal to the number of incorporated atoms in the island $Ld\theta$, one can integrate Eq. (3) as

$$C_i(\theta) = 1 - \left(1 - \frac{\theta}{2}\right)\alpha. \tag{4}$$

Equation (4) is represented by a dot-dashed line in Fig. 7(b) for α=0.71. Except for the initial Cu deposition of 0.11 ML, the experimental Cu fractions are always higher than this simple kinetic model. This indicates that other Cu source should be taken into account to enhance the Cu fraction. We assumed that buried Cu atoms underneath the island were lifted to the topmost layer during the island growth. If all buried Cu are incorporated into the top layer, Eq. (4) should be

$$C_i(\theta) = 1 - (1-\theta)\alpha. \tag{5}$$

In this case, all deposited Cu will cover the entire surface for 1 ML Cu deposition. Equation (5) is represented by a broken line for α=0.71, and fairly reproduced but slightly overestimated the experimental result for the Cu coverage of more than 0.6 ML. Of course this kinetic model is too simple to correctly reproduce the experimental Cu fraction, particularly on the point where the surface should be close to thermal equilibrium. However, lifting the buried Cu will apparently play an important role in enriching the Cu fraction on the island.

Still an unresolved feature is the initial suppression of Cu on the island, as was indeed observed in Fig. 2. One possible origin of this initial Ni-rich island is a result of phase separation between Ni and Cu for low Cu concentration. It has been pointed out that the Cu-Ni alloy will be a possible spinodal decomposition at a fairly low temperature because enthalpy of alloy formation H_m is positive.[5,31,35,36] The value of H_m is, however, small, and the decomposition temperature is low compared to the bulk diffusion limit, therefore, practically no phase separation will be expected for bulk Cu-Ni alloy. On the surface, H_m would be enhanced[37] and migration of surface atoms at low temperatures would further promote phase separation. An interesting observation was that even though islands had the same width, Cu fractions were completely different between 0.11 and 0.20 ML depositions. This indicates that the Cu suppression on the island for the initial Cu deposition will not be simply caused by the local stress such as seen for the local order around the dislocation.[38]

IV. CONCLUSION

We have shown that, in contrast to Ni(111) and Ni(001) surfaces, Ni(110) surface exhibited significant Cu mixing into the substrate and the island for the initial overlayer formation even at room temperature. This is partly due to the open geometry of the fcc(110) 1×1 surface structure promoting Cu/Ni exchange, and partly due to the migration of Cu and Ni on the surface even at room temperature, which is suggested by successive STM images. Quantitative Cu fraction measurements showed that about 0.71 ± 0.04 of deposited Cu squeezed out substrate Ni, revealed by atom-resolved STM images. Cu enrichment was observed on the island, suggesting embedded Cu is lifted into the top layer by Cu/Ni replacement during lateral island growth. The driving force of the Cu lifting is an energetic gain compared to the Ni surface, and this is indeed kinetically driven surface segregation by the island formation rather than thermal movement. Finally, discrimination of individual Cu and Ni on the surface by STM enables us to offer unexpected and new insights into the classical Cu/Ni alloy formation.

*tfukuda@a-phys.eng.osaka-cu.ac.jp

[1] *The Chemical Physics of Solid Surfaces*, Surface Alloys and Alloy Surfaces Vol. 10, edited by D. P. Woodruff (Elsevier, Amsterdam, 2002).
[2] L. Pleth Nielsen, F. Besenbacher, I. Stensgaard, E. Lægsgaard, C. Engdahl, P. Stoltze, K. W. Jacobsen, and J. K. Nørskov, Phys. Rev. Lett. **71**, 754 (1993).
[3] P. M. Holmblad, J. H. Larsen, I. Chorkendoff, L. P. Nielsen, F. Besenbacher, I. Stensgaard, E. Lægsgaard, P. Kratzer, B. Hammer, and J. K. Nørskov, Catal. Lett. **40**, 131 (1996).
[4] P. T. Sprunger, E. Lægsgaard, and F. Besenbacher, Phys. Rev. B **54**, 8163 (1996).
[5] F. Besenbacher, L. P. Nielsen, and P. T. Sprunger, *The Chemical Physics of Solid Surfaces*, Growth and Properties of Ultrathin Epitaxial Layer Surface Vol. 8 (Elsevier, Amsterdam, 1997), Chap. 6.
[6] K. Wandelt and C. R. Brundle, Phys. Rev. Lett. **46**, 1529 (1981).
[7] P. R. Webber, M. A. Morris, and Z. G. Zhang, J. Phys. F: Met. Phys. **16**, 413 (1986).
[8] K. Amemiya, E. Sakai, D. Matsumura, H. Abe, T. Ohta, and T. Yokoyama, Phys. Rev. B **71**, 214420 (2005).
[9] A. Chambers and D. C. Jackson, Philos. Mag. **31**, 1357 (1975).
[10] B. Müller, B. Fischer, L. Nedelmann, A. Fricke, and K. Kern, Phys. Rev. Lett. **76**, 2358 (1996).
[11] B. Müller, L. Nedelmann, B. Fischer, A. Fricke, and K. Kern, J. Vac. Sci. Technol. A **14**, 1878 (1996).
[12] S. A. Chambers, H. W. Chen, I. M. Vitomirov, S. B. Anderson, and J. H. Weaver, Phys. Rev. B **33**, 8810 (1986).
[13] W. F. Egelhoff, Jr., J. Vac. Sci. Technol. A **2**, 350 (1984).
[14] W. F. Egelhoff, Jr., Phys. Rev. B **30**, 1052 (1984).
[15] E. L. Bullock and C. S. Fadley, Phys. Rev. B **31**, 1212 (1985).
[16] F. B. Rasmussen, J. Baker, M. Nielsen, R. Feidenhans'l, and R. L. Johnson, Phys. Rev. Lett. **79**, 4413 (1997).
[17] J. Voigt, X. L. Ding, R. Fink, G. Krausch, B. Luckscheiter, R. Platzer, U. Wöhrmann, and G. Schatz, Phys. Rev. Lett. **66**, 3199 (1991).
[18] G. Held, W. Sklarek, M. Mayan, and H.-P. Steinrück, Surf. Sci. **402-404**, 322 (1998).
[19] X. H. Feng, M. R. Yu, S. Yang, G. Meigs, and E. Garfunkel, J. Chem. Phys. **90**, 7516 (1989).
[20] Th. Berghaus, Ch. Lunau, H. Neddermeyer, and V. Gogge, Surf. Sci. **182**, 13 (1987).
[21] V. Rogge and H. Neddermeyer, Phys. Rev. B **40**, 7559 (1989).
[22] N. Memmel, E. Lægsgaard, I. Stensgaard, and F. Besenbacher, Phys. Rev. B **72**, 085411 (2005).
[23] G. Ertl and K. Wandelt, Phys. Rev. Lett. **29**, 218 (1972).
[24] P. W. Murray, S. Thorshaug, I. Stensgaard, F. Besenbacher, E. Lægsgaard, A. V. Ruban, K. W. Jacobsen, G. Kopidakis, and H. L. Skriver, Phys. Rev. B **55**, 1380 (1997).
[25] J. Lindner, P. Poulopoulos, F. Wilhelm, M. Farle, and K. Baberschke, Phys. Rev. B **62**, 10431 (2000).
[26] M. Schmid, H. Stadler, and P. Varga, Phys. Rev. Lett. **70**, 1441 (1993).
[27] R. T. Tung and R. Graham, Surf. Sci. **97**, 73 (1980).
[28] G. L. Kellogg, Phys. Rev. Lett. **67**, 216 (1991).
[29] http://cms.mpi.univie.ac.at/vasp/vasp/vasp.html
[30] D. Spišák and J. Hafner, J. Phys.: Condens. Matter **12**, L139 (2000).
[31] W. M. H. Sachtler and P. Van Der Plank, Surf. Sci. **18**, 62 (1969).
[32] T. Fukuda and H. Nakayama (unpublished).
[33] T. Fukuda, K. Iwamoto, K. Umezawa, and H. Nakayama (unpublished).
[34] W. M. H. Sachtler and R. Jongepier, J. Catal. **4**, 654 (1965).
[35] W. M. H. Sachtler and R. Jongepier, J. Catal. **4**, 665 (1965).
[36] T. Sakurai, T. Hashizume, A. Jimbo, A. Sakai, and S. Hyodo, Phys. Rev. Lett. **55**, 514 (1985).
[37] J. L. Morán-López and L. M. Falicov, Phys. Rev. B **18**, 2549 (1978).
[38] G. Ritz, M. Schmid, A. Biedermann, and P. Varga, Phys. Rev. B **53**, 16019 (1996).